Naveen Kumar Verma, Prateek Khare and Nishith Verma*

Synthesis of iron-doped resorcinol formaldehyde-based aerogels for the removal of Cr(VI) from water

Abstract: Iron-doped resorcinol formaldehyde-based aerogels (Fe-RF-AGs) were synthesized and used for the removal of hexavalent chromium [Cr(VI)] from water using adsorption. The synthesis steps of Fe-RF-AGs comprised the gelation by the polycondensation of resorcinol and formaldehyde, followed by drying using supercritical carbon dioxide. The produced mesoporous material was *in situ* doped with iron (Fe) before the incipience of gel formation, using ferrocene as the metal precursor. Various analytical techniques were used to characterize the prepared materials. The batch adsorption study was performed containing different amounts of Fe in the gel, different initial Cr(VI) concentrations of the solution, and at different solution pH and temperatures. The adsorption rate was found to be first order. The equilibrium data were explained using the Freundlich isotherm. The thermodynamic calculations revealed that the adsorption of Cr(VI) was spontaneous, endothermic and irreversible over the temperature range of 20–40°C. The maximum adsorption capacity of Fe-RF-AGs for Cr(VI) was found to be approximately 55 mg/g at 30°C at the aqueous phase concentration of 275 mg/l, which is larger than most of the data discussed in the literature. The results indicated that Fe-RF-AGs can be used as an effective adsorbent for the removal of Cr(VI) ions from waste water.

Keywords: adsorption; chromium(VI); Fe-doping; RF aerogels; waste water treatment.

DOI 10.1515/gps-2014-0072
Received September 26, 2014; accepted November 28, 2014; previously published online January 21, 2015

***Corresponding author: Nishith Verma,** Indian Institute of Technology Kanpur, Department of Chemical Engineering, Kanpur 208016, India; and Center for Environmental Science and Engineering, Indian Institute of Technology Kanpur, Kanpur 208016, India, e-mail: vermanishith@gmail.com
Naveen Kumar Verma and Prateek Khare: Indian Institute of Technology Kanpur, Department of Chemical Engineering, Kanpur 208016, India

1 Introduction

Chromium (Cr) is one of the most abundant elements and major pollutants in industrial effluents, responsible for the contamination of water resources globally [1]. The contamination of groundwater with Cr ions can be detrimental to plant growth and also, to the health of animals [2]. Cr ions exist in two natural forms: hexavalent chromium [Cr(VI)] and trivalent chromium [Cr(III)]. The former ions are present as chromate ($CrO4^{2-}$) and dichromate ($Cr_2O_7^{2-}$) in water and are more hazardous to human being than the latter [3]. The permissible limit of Cr(VI) ions in industrial waste water effluents and drinking water are 0.1 mg/l and 0.05 mg/l, respectively, as per the World Health Organization (WHO) [4]. There is a necessity of treating Cr-laden industrial effluents before discharging them to the water bodies.

Various conventional methods have been used for the remediation of Cr(VI)-laden water, such as electro-dialysis, oxidation/reduction, chemical precipitation, evaporation, reverse osmosis, filtration, ion exchange, solvent extraction and adsorption [5–10]. A relatively larger capital and operative costs, and problems associated with the disposal of the residual sludge are major drawbacks of the conventional methods such as electro-dialysis, oxidation/reduction, chemical precipitation, evaporation, reverse osmosis, filtration, ion exchange, and solvent extraction. These methods may also produce a toxic sludge, the handling, storage, and treatment of which can be expensive. On the contrary, adsorption is considered to be energy-efficient, environmentally benign, economically feasible, and a simple and effective process for the removal of contaminants at relatively lower concentration levels. Further, the used adsorbents can be regenerated under controlled operating conditions to produce a sludge which has high metal concentrations. Such sludge may be processed to recover metals or generate useful products.

Several natural and synthetic materials such as activated carbon, chitosan, polyaniline, polypyrrole, silica, zeolite, clay, and metal oxides-based composites have been used for the removal of Cr(VI) from aqueous

solutions [5, 6, 10–14]. Recently, aerogels (AGs) are being used for environmental remediation applications because of their unique physico-chemical characteristics such as large internal surface area and high porosity, which are desirable for effective adsorption [14–18].

Resorcinol-formaldehyde-based aerogels (RF-AGs) are porous materials. They are amenable to surface functionalization which may enhance the adsorption capacity of the materials. RF-AGs are produced by the polycondensation of resorcinol and formaldehyde in acidic or basic solvent, followed by drying under controlled conditions to minimize the shrinkage and collapse of the porous matrix [19]. The supercritical CO_2 drying is generally used for drying of aerogels to produce a stable porous structure.

The previous versions of RF-AGs were synthesized in a base-catalyzed aqueous medium. The major drawback of base-catalyzed methods is a relatively longer gelation time (up to 7 days at 85°C). Recently, different acids such as perchloric acid- [20], nitric acid- [21], and acetic acid-catalyzed RF-aerogels [22] have been synthesized with gelation times varying between one to three days at 45–80°C. However, the hydrogen chloride (HCl) catalyzed RF-AGs were prepared in approximately 2 h at room temperature (~30°C) and in 10 min at 80°C, which may be considered to be one of the best methods reported in the literature [23, 24]. RF-AGs have also been doped with different metals such as copper, nickel, cobalt and iron [25, 26].

In the present study, HCl catalyzed Fe-doped RF-AGs (Fe-RF-AGs) were synthesized using the polycondensation of resorcinol and formaldehyde in acetonitrile to produce gels, followed by drying using supercritical CO_2. The novelty lies in the synthesis of Fe-RF-AG aerogels. The metal precursor (ferrocene) was incorporated *in situ* during a synthesis step and the prepared material was used as an adsorbent for Cr(VI). To our knowledge, the *in situ* Fe-doped RF-AG aerogels have been used for the first time as an adsorbent for Cr(VI) in this study. Fe has an affinity for Cr(VI) ions, producing Cr-Fe complexes [27]. The experimental results, discussed later, demonstrated that the material was a potential adsorbent for the removal of Cr(VI) ions from waste water.

The synthesized Fe-RF-AGs were characterized using different analytical techniques such as the Brunauer-Emmett-Teller (BET) area and pore-size-distribution (PSD) measurement, scanning electron microscopy (SEM), energy dispersive X-ray (EDX), atomic absorption spectroscopy (AAS) and Fourier transform infrared spectroscopy (FTIR). The batch adsorption tests were performed under different operating conditions such as Fe contents in the produced adsorbents, adsorbent-dosage, adsorption (contact) time, initial concentrations of Cr(VI) in water, and pH. The kinetic and thermodynamic parameters were extracted from the experimental data.

2 Materials and methods

2.1 Materials

Resorcinol ($C_6H_4(OH)_2$, 99%), formaldehyde (HCHO, 37%), hydrochloric acid (HCl, 35%), acetonitrile (CH_3CN, 99%), 1-5-diphenylcarbazide ($C_{13}H_{14}N_4O$) and sodium hydroxide (NaOH, 97%) were purchased from Merck (Darmstadt, Germany). Ferrocene ($(C_5H_5)_2Fe$, 98%), acetone ($(CH_3)_2CO$, 99%), and potassium dichromate ($K_2Cr_2O_7$, 99.5%) were purchased from Sigma Aldrich (St. Loius, MO, USA). Carbon dioxide (CO_2) was purchased from Sigma Gases (Delhi, India). All aqueous solutions used in this study were prepared in Milli-Q (Aqua Guard, Millipore, WA, USA) water.

2.2 Synthesis of RF-AG and Fe-RF-AG

Figure 1 shows the schematic illustration of the synthesis steps for Fe-RF-AGs. The steps are the same as those used by Mulik et al. [24]. As a modification of this method, ferrocene was used as the iron precursor, and added i*n situ* before the curing step (gel formation) to produce Fe-RF-AG. Resorcinol (0.334 g), hydrochloric acid (30 µl) and formaldehyde (480 µl) were mixed with 13 ml ofacetonitrile solution contained in a polypropylene mold to produce a homogenous solution. Ferrocene was added in different amounts (10, 20, 30, 40 and 50 mol%

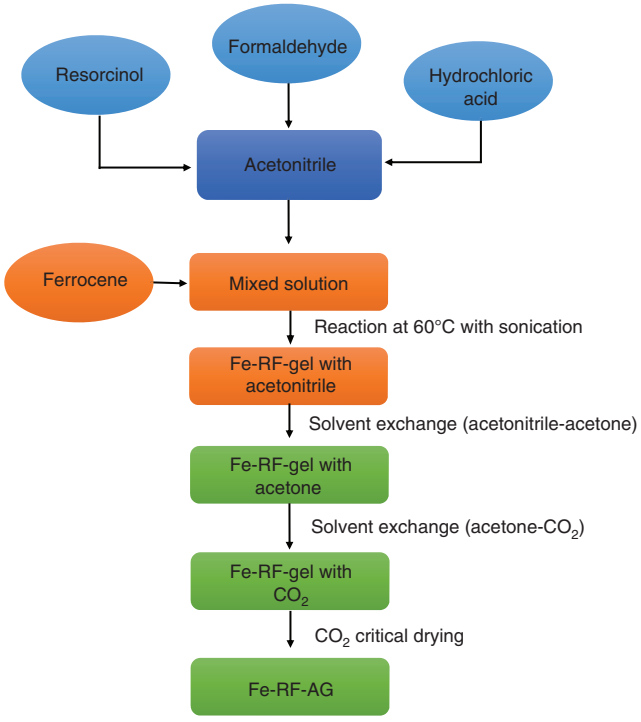

Figure 1 Schematic illustration of the synthesis of Fe-RF-AGs.

with respect to resorcinol) to the homogenous solution, as a Fe-doping agent. Next, the solution was heated to 60°C. It took about 2 min to reach 60°C from room temperature (35°C). The solution was then ultrasonicated for 10 min, keeping the temperature constant at 60°C. Some gel samples were prepared without incorporating Fe. After sonication, RF or Fe-RF gels were produced. The acetonitrile contained in the pores of the gel was exchanged with 50 ml of acetone at room temperature (35°C), and replaced with fresh acetone at the regular intervals of 8 h. This exchange process took approximately 48 h for completion. Next, the RF/Fe-RF gel sample containing acetone in its pores was kept in a sampler placed in the autoclave, as shown in the schematic illustration (Figure 2) of the setup used for the supercritical drying of the gel samples. The sampler was filled with liquid CO_2 and kept for 24 h to replace acetone with the liquid at 20°C. The autoclave was then heated to 32°C at 73 bar for achieving the supercritical conditions. Next, the sampler was depressurized by venting CO_2 at 40°C and the porous RF-AG or Fe-RF-AG was produced. Figure 3 shows the photos of different gels and aerogels with and without Fe produced in this study. Different colors of the materials doped with and without Fe are observed.

It is important to mention that water is commonly used as a solvent for gel preparation. In this study, acetonitrile was used as a solvent instead of water to disperse ferrocene, as in the method of Mulik et al. [24]. Acetonitrile acted as a polymerization medium only. It did not participate in the reaction. However, gel formation occurred very fast (within 10 min) in acetonitrile compared with water (in 5 days). Moreover, the produced gel retained the shape of pores in Fe-RF-AG prepared using acetonitrile. On the contrary, the pores shrunk when water was used as the solvent.

2.3 Batch adsorption study

The Cr(VI) solutions of different concentrations were prepared using a stock solution of 1000 mg/l concentration by dissolving $K_2Cr_2O_7$ salt in water. All adsorption experiments were performed in conical flasks containing 50 ml of Cr(VI) solution and the adsorbents. The flasks were placed in an orbital shaker incubator. The speed was set at 150 rpm. Next, the adsorbent was separated from the solution using a filter paper (Whatman ashless filter paper; grade no. 42; diameter: 125 mm). The concentration of Cr(VI) in the test solution was determined using 1,5-diphenylcarbazide (DPC) method [28]. Approximately 0.5 g-DPC was mixed in 100 ml of acetone, which was then stored in a glass bottle at 4°C in the dark. Approximately 5 ml of the prepared solution was mixed with a 7.5 ml of water-H_2SO_4 (1:1 v/v) solution. Next, 0.12 ml of the prepared developer solution was mixed with 5 ml of Cr(VI) solution. A coloured Cr(VI) metal-complex was produced. The metal analysis of the solution was performed using the UV-Vis double beam-spectrophotometer (Carry 100 Bio, Varian, USA) and a characteristic peak was detected at 540 nm-wavelength. The intensity of the peak increased with increasing Cr(VI) concentrations up to 3 ppm. The batch adsorption tests were performed for different adsorbent doses, contact times, pH and Fe contents in the adsorbents. The pH of the solutions was adjusted using 0.1 M HCl and 0.1 M NaOH solutions. The percentage removal of Cr(VI) from the aqueous solution was determined from the data:

$$\%\text{Removal}=\frac{C_0-C_e}{C_0}\times 100, \tag{1}$$

where C_0 and C_e are the concentrations of Cr(VI) before and after adsorption, respectively. To estimate the uptake (q_e, mg/g) of Cr(VI) on the adsorbent, the following equation was used:

$$q_e=\frac{C_0-C_e}{w}\times V, \tag{2}$$

where w (g) and V (L) are the amounts of the adsorbent and the volume of Cr(VI) solution used for adsorption tests, respectively.

2.4 Adsorbent characterization

The Fe-RF-AG samples were characterized for their physico-chemical surface characteristics using different analytical techniques. The surface morphology of the synthesized materials was observed using a field emission scanning electron microscope (FE-SEM) (Gemini Supra 40 VP, Zeiss) after the gold coating of the samples. The elemental compositions of the samples were determined using EDX (Oxford, Inca, Germany) and the area scanning of different locations in the sample. The BET surface area and the PSD of the prepared samples

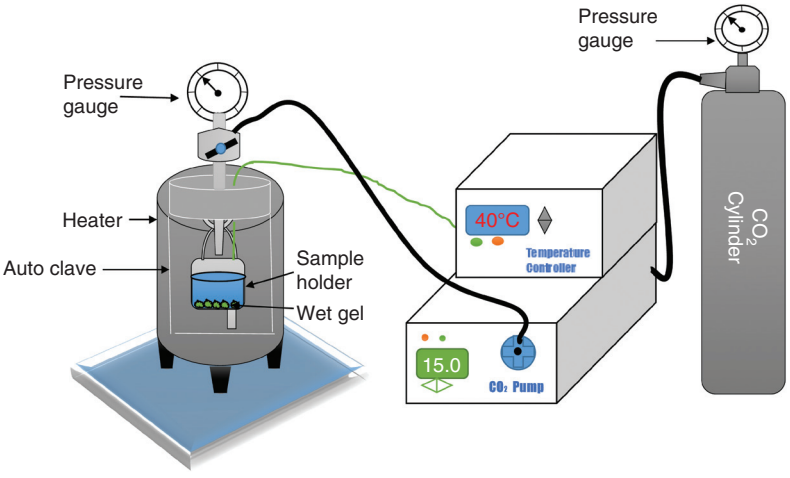

Figure 2 Schematic illustration of the supercritical CO_2 drying setup.

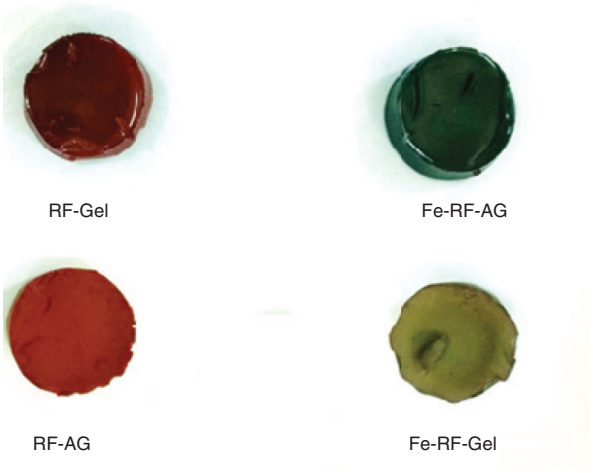

Figure 3 Photos of the synthesized samples: RF-Gel, Fe-RF-Gel, RF-AG and Fe-RF-AG.

were determined using N_2 at 77 K and the Autosorb-1C instrument (Quantachrome, USA). The samples were degassed for 12 h to remove moisture prior to the analysis. The BET surface area was calculated from the linear segment (P/P_o from 0.05 to 0.35) of the N_2 adsorption isotherm. The total pore volume was determined from the amount of N_2 adsorbed at a relative pressure near unity (0.9994). The meso- and micro-pore volumes were determined using the Barrett-Joyner-Halenda (BJH) method and the density functional theory (DFT), respectively. Prior to the analysis, the samples were degassed at 120°C under vacuum for several hours. The FTIR spectra (Bruker Tensor 27, Germany) were obtained to determine the surface functional groups of the prepared samples before and after exposure to the Cr(VI) solution. The spectra were recorded over the wave number-range of 1000–4000 cm^{-1} with 20 scans per sample, using attenuated total reflectance (ATR) with a germanium (Ge) crystal.

3 Results and discussion

3.1 Adsorbent characterization

3.1.1 AAS analysis

Fe contents in the prepared samples were determined using the AAS (Varian AA-240, USA) analysis. The Fe-RF-AG samples were crushed using mortar and pestle and digested in aqua regia to leach out the metal particles. Table 1 summarizes the Fe loading in different Fe-RF-AG samples. The metal loading increased approximately two times on increasing the molar concentration of ferrocene from 10 to 30% *in situ* incorporated in the polymeric matrix during synthesis (before gel formation). The increase in the metal loading at concentrations >30% was found to be insignificant. At relatively higher concentrations, metal particles were unbound to the polymeric gel matrix and leached out during the solvent exchange process. Based on the AAS data, all samples were prepared using 30% molar concentration of ferrocene.

Table 1 Fe loadings in the synthesized aerogel samples using AAS.

Fe (% molar concentration) in Fe-RF-AG	Fe loading (mg/g)
10	7.15
20	10.0
30	14.10
40	15.20
50	16.41

3.1.2 SEM analysis

SEM images were taken at 50 kx magnification to observe the surface morphology of the prepared samples. Figure 4A shows the porous structure of the RF-AG sample. Figure 4B shows the porous texture of Fe-RF-AG, with some localized agglomeration of the metals observed on the surface, attributed to a few unbounded Fe contents in the RF-AG matrix. Here, it may be mentioned that the *in situ* doping of RF-AG before the curing step resulted in a physical dispersion of the Fe contents within the gel matrix during curing. The unbound Fe contents in the gel appeared in the form of a few patches as observed in Figure 4B. Therefore, the dispersion of Fe contents within the gel matrix was only physical and ferrocene did not participate in the polycondensation reaction between resorcinol and formaldehyde. Figure 4C shows the surface of the Fe-RF-AG samples after the adsorption with Cr(VI). A distinct change in the surface morphology was observed, with the surface covered with Cr(VI). Figure 4A′, B′, C′ show the area-EDX spectra of the RF-AG, Fe-RF-AG and Cr(VI)-adsorbed Fe-RF-AG samples, respectively. The spectra confirmed the presence of Fe before adsorption and that of Fe and Cr in Fe-RF-AG after adsorption with Cr(VI). In Figure 4B′, C′, the appearance of gold-peak was attributed to the gold coating of the samples before the EDX analysis.

3.1.3 BET analysis

Table 2 summarizes the BET surface area, macro-, meso-, micropore volumes and total pore volume of the RF-AG, Fe-RF-AG samples. The generation of porosity in RF-AG was attributed to the solvent exchange and the evaporation of the solvent from the material during supercritical

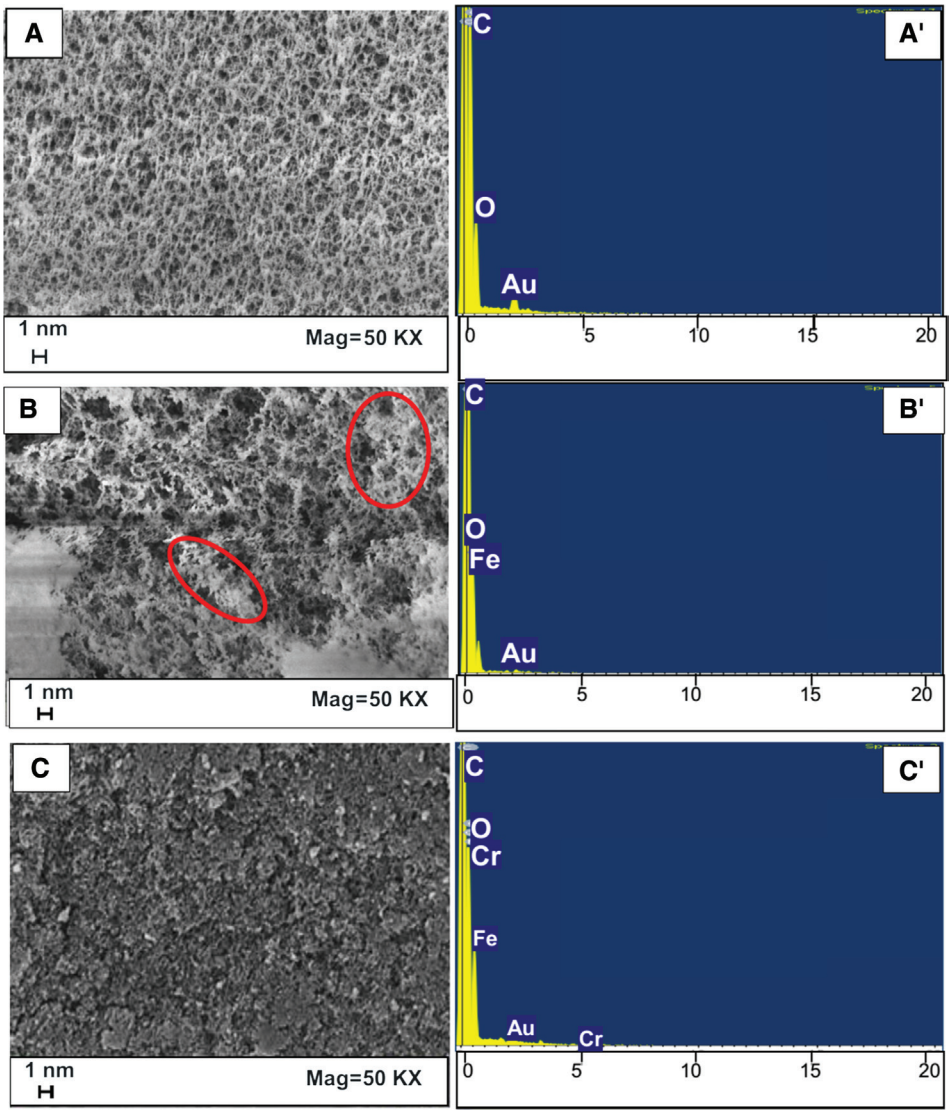

Figure 4 SEM and EDX spectra of different samples: (A, A′) RF-AG, (B, B′) Fe-RF-AG, and (C, C′) Cr(VI)-adsorbed Fe-RF-AG.

Table 2 BET area and pore volumes of aerogels.

Adsorbents	BET surface area (m^2/g)	Total pore volume (ml/g)	Macro pore volume (ml/g)	Meso pore volume (ml/g)	Micro pore volume (ml/g)
RF-AG	341.1	1.014	0.442	0.496	0.075
Fe-RF-AG (Fe 10%)	248.1	0.626	0.212	0.346	0.067
Fe-RF-AG (Fe 30%)	224.2	0.499	0.141	0.298	0.060

drying. The BET surface area of RF-AG was determined to be 341 m^2/g. The surface area and porosity decreased with increase in the Fe contents that were incorporated *in situ* during synthesis. The decrease was attributed to the presence of the unbound Fe contents present in the materials even after the supercritical drying. Such unbound Fe contents in Fe-RF-AG were observed as agglomerated species in the SEM image shown in Figure 4B.

3.1.4 FTIR spectra

Figure 5 shows the FTIR spectra of Fe-RF-AGs. The peaks at ~3260 and ~3645 cm^{-1} were attributed to –OH groups, whereas that at ~1700 cm^{-1} was attributed to the aromatic C=C stretch of resorcinol used in the synthesis. The peak at ~2360 cm^{-1} corresponded to the presence of CO_2 on the surface of the material and it appeared because of the

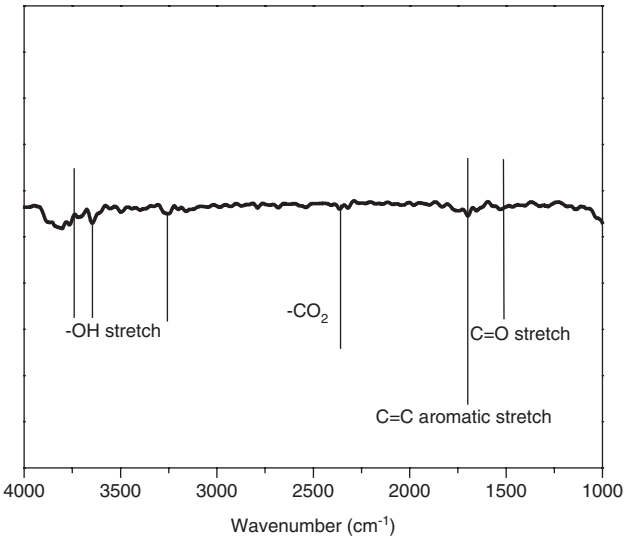

Figure 5 FTIR spectra of Fe-RF-AG.

drying of the material using the supercritical CO_2. The peak at ~1510 cm^{-1} was attributed to the C=O (aliphatic ketone) stretch of acetone.

3.2 Batch adsorption study

3.2.1 Effect of Fe loading in adsorbents

Figure 6 shows variation in Cr(VI) uptake in the RF-AG adsorbents containing different Fe contents (10–50% molar concentrations of ferrocene). The uptake increased with increasing Fe contents in the RF-AG matrix. However, the materials synthesized using 30% or more concentrations exhibited a similar adsorption capacity, with <4% increase observed in the capacity. The results are consistent with the Fe loadings shown in Table 1 for the different Fe-RF-AG samples. The increase in the adsorption capacity of the material with increasing Fe loadings in the AG matrix confirmed the affinity of the Fe toward Cr(VI).

3.2.2 Effect of adsorbent dose and time

The effect of adsorbent dose was studied using different amounts (0.02–0.3 g) of adsorbent in 50 ml of 100 mg/l of Cr(VI) solution at 30°C for 24 h. Figure 7 shows that the percentage removal of Cr increased with increasing adsorbent dosages and attained a maximum level. Approximately 0.2 g of the dosage was found to be effective, with 98–99% Cr-removal and ~25 mg/g of Cr(VI) uptake. The results also indicated that the specific uptake (mg/g) of Cr(VI) ions on the adsorbent decreased with increasing adsorbent doses. Hereafter, all experiments were performed using a 0.2 g adsorbent dose.The effect of contact times on the percentage removal of the solute was investigated by varying contact time and keeping the other parameters constant. The percentage removal of Cr(VI) gradually increased with increasing contact times. There was no significant change observed in the percentage removal at ~24 h or after.

3.2.3 Effect of pH

The adsorption of Cr(VI) on Fe-RF-AG can be rendered relatively larger or smaller by adjusting the initial pH

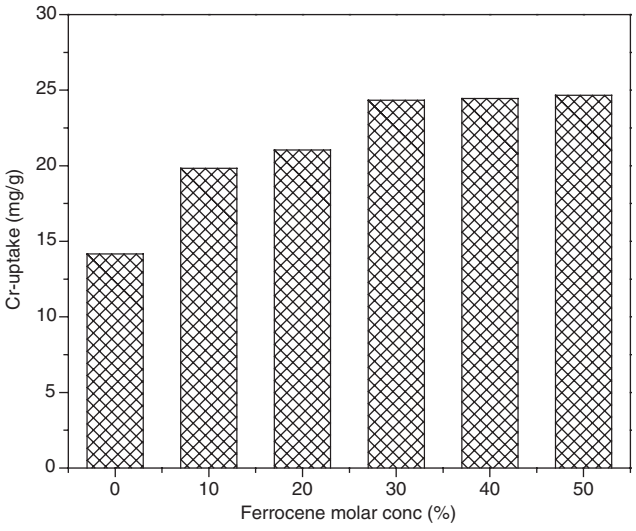

Figure 6 Effect of Fe loading on the adsorption of Cr(VI) (initial concentration=100 mg/l, weight=0.2 g, temperature=30°C, time=24 h).

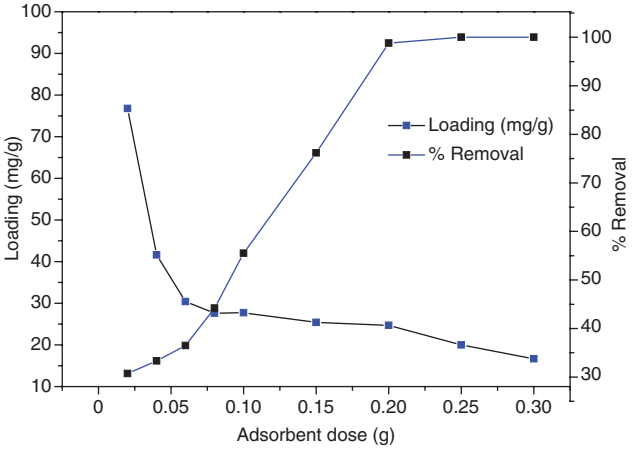

Figure 7 Effect of adsorbent dose on the adsorption of Cr(VI) (initial concentration=100 mg/l, temperature=30°C, time=24 h).

of the solutions, because of the interactions of Cr(VI) ions with the surface functional groups on Fe-RF-AG. The effect of initial pH on the adsorption capacity was investigated by adjusting initial pH (1–10) of a 500 mg/l of Cr(VI) solution. Figure 8 shows that the maximum adsorption uptake (~125 mg/g) was observed at pH=~2. The uptake considerably decreased on increasing pH because of the competitive adsorption of OH^- ions relative to Cr(VI) ions.

3.3 Adsorption kinetics modeling

Different kinetic models were used to investigate the adsorption kinetics of Cr(VI) on Fe-RF-AGs. The first order equation is generally expressed as

$$-\frac{dC_t}{dt}=k_1C_t \tag{3}$$

Here, C_t is the solution concentration at time t and k_1 is the first order adsorption rate constant (min^{-1}). Equation (3) can be integrated to obtain a more useful form of the equation:

$$\ln(C_t)=\ln(C_0)-k_1t \tag{4}$$

The plot of $\ln(C_t)$ vs. t is linear and k_1 can be determined from the slope. The first order kinetic equation was found to fit the adsorption data for Cr(VI) on Fe-RF-AGs reasonably well. The correlation coefficients (R^2) and the rate constant were found to be 0.984 and 0.0021 min^{-1}, respectively. A relatively lower R^2 value, equal to 0.76, was obtained in the case of the second order kinetic equation.

3.4 Adsorption isotherms

The equilibrium adsorption isotherm shows the relationship between the amounts of a solute adsorbed per unit mass of the adsorbent in equilibrium with the solution at a constant temperature. The Langmuir isotherm describes the monolayer adsorption of a solute on the homogeneous surface. The model assumes uniformly energetic sites on the surface. The Freundlich isotherm allows for the multilayer adsorption and the model is applicable for the adsorption on a heterogeneous surface having a non-uniform energy distribution of the active sites. The adsorption isotherm for Cr(VI) on Fe-RF-AG was determined from the adsorption tests performed using the Cr(VI) solutions of different initial concentrations and the fixed dose (0.2 g) of the adsorbent. All tests were performed at 30°C. Figure 9 shows the equilibrium loading and the linearized form of the Freundlich isotherm for the adsorption of Cr(VI) on Fe-RF-AG. The adsorption capacity of the prepared material was determined to be ~55 mg/g at the equilibrium concentration of 270 ppm. The inset in Figure 9 shows the fitting of the experimental data with the Freundlich equation. A reasonably good fit was observed. The corresponding results for the Langmuir isotherm are not included for brevity. Table 3 presents the linearized forms of Langmuir and Freundlich isotherm equations, the correlation coefficients (R^2), and the isotherm parameters calculated from the isotherm equations fitted to the adsorption data. In the linearized Langmuir model, q_e represents the monolayer equilibrium uptake of Cr(VI) adsorbed per unit amount of the adsorbent, C_e represents the metal residual concentration in the solution, q_{max} denotes the maximum specific

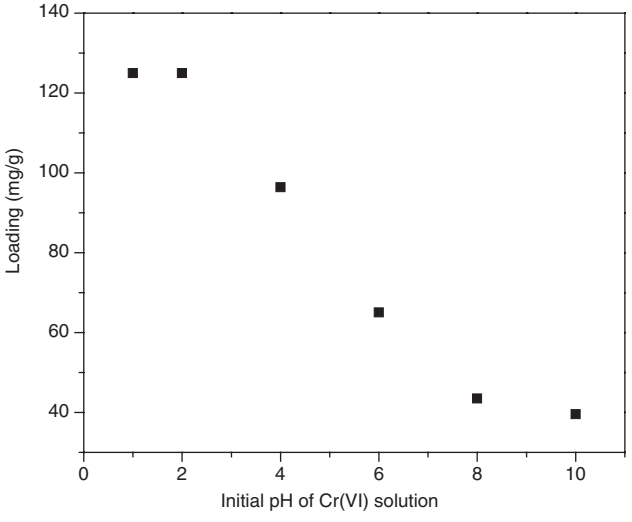

Figure 8 Effect of pH on the adsorption of Cr(VI) (initial concentration=500 mg/l, weight=0.2 g, temperature=30°C, time=24 h).

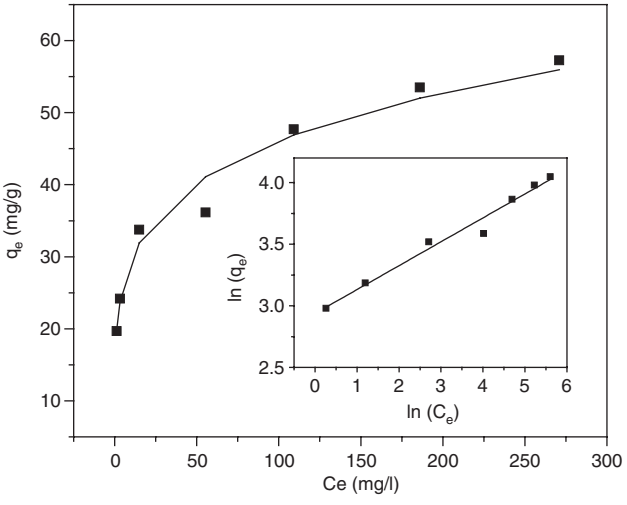

Figure 9 Equilibrium loading and linearized Freundlich isotherm for the adsorption of Cr(VI) on Fe-RF-AG.

Table 3 Isotherms and statistical parameters.

Langmuir $\frac{1}{q_e}=\frac{1}{k_l q_{max} C_e}+\frac{1}{q_{max}}$		Freundlich $\ln q_e - \ln k_f = \frac{1}{n}\ln C_e$	
q_{max} (mg/g)	43.859	$1/n$	0.194
K_l (l/mg)	0.5657	K_f	18.872
R^2	0.853	R^2	0.978

uptake of the adsorbent, and K_l is the Langmuir constant. In the linearized Freundlich isotherm, K_f is the Freundlich constant, n is the adsorption intensity, q_e is the amount of Cr(VI) adsorbed in multilayer at equilibrium and C_e is the equilibrium concentration of Cr(VI) in the solution. The R^2 value of 0.978 for the Freundlich isotherm equation, being closer to unity, confirmed the applicability of the Freundlich isotherm for the adsorption of Cr(VI) on the prepared adsorbents. On the contrary, the R^2 value of 0.853 for the Langmuir isotherm equation, being far from unity indicated a non-linear fit, and therefore, the non-applicability of the Langmuir isotherm. The adsorption capacity of Fe-RF-AGs was also compared with a few Fe-based adsorbents discussed in the literature for Cr(VI) and found to be larger in most cases [29–34]. Table 4 lists such comparative data.

3.5 Adsorption thermodynamics

The temperature dependence of adsorption may be described using three thermodynamic parameters, namely, change in the Gibb's free energy (ΔG), entropy of adsorption (ΔS) and enthalpy of adsorption (ΔH). The Van't Hoff equation relates ΔG to the adsorption equilibrium constant as follows:

$$\Delta G = -RT\ln(K_D), \tag{5}$$

where K_D is the equilibrium constant; R is the universal gas constant and T is absolute temperature. The equilibrium constant may be calculated from solution concentrations:

$$K_D = \frac{C_0 - C_e}{C_e}, \tag{6}$$

where C_0 and C_e are initial and equilibrium concentrations in the solution, respectively. ΔG may also be written in terms of ΔH and ΔS:

$$\Delta G = \Delta H - T\Delta S \tag{7}$$

On substituting equation (7) in equation (5) and rearranging, the following equation is obtained:

$$\ln(K_D) = -\frac{\Delta H}{RT} + \frac{\Delta S}{R} \tag{8}$$

Figure 10 shows a good linear fit of the adsorption data with the Van't Hoff equation. The numerical value of ΔS equal to or more than zero indicates that the process is irreversible. A negative value of ΔG denotes the spontaneity of the process. In our study, the values of ΔS and ΔG were found to be positive and negative, respectively (Table 5), indicating that the adsorption of Cr(VI) was irreversible and spontaneous.

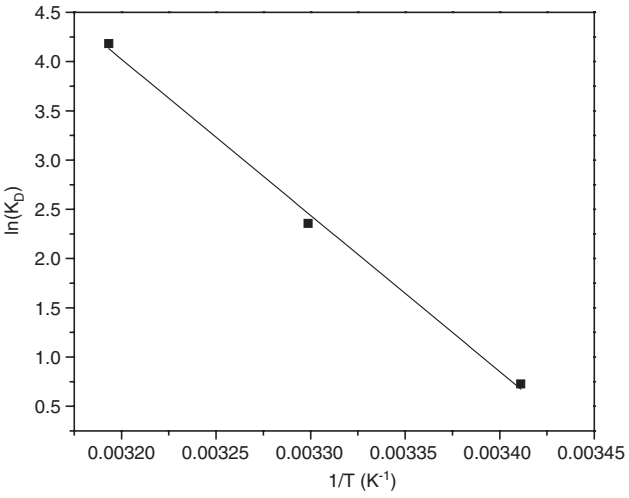

Figure 10 Van't Hoff equation plot for the adsorption of Cr(VI) on Fe-RF-AG.

Table 4 Fe-based adsorbents for Cr(VI) removal.

S. No.	Adsorbent	C (ppm)	q_{max} (mg/g)	References
1	Fe-RF-AG	2–270	55	This study
2	Iron-doped carbon beads	10–150	45	[29]
3	Iron-doped in orange peel pith	10	5.37	[30]
4	Mesoporous magnetic γ-Fe_2O_3	50	15.6	[31]
5	nZVI-Fe_3O_4 nanocomposites	20–80	29, 100	[32]
6	Iron (Fe^{+3}) oxide/hydroxide suspension	10–50	45.32	[33]
7	Iron-nickel oxide magnetic particles	10–50	33.44	[34]

Table 5 Thermodynamic parameters.

T (°C)	ln(K_c)	$\Delta G = -RT \ln(K_c)$ (kJ/mol)	ΔH (kJ/mol)	ΔS (kJ/mol-K)
20	0.725	-1.767	131.818	0.455
30	2.356	-5.940		
40	4.182	-10.889		

4 Conclusions

Resorcinol- and formaldehyde-based porous aerogels (~225 m^2/g) were successfully synthesized using HCl acid catalyst and supercritical CO_2 drying. Fe was *in situ* incorporated in the gel at the incipience of gel formation, using ferrocene as the precursor for Fe. The ability of the produced materials to remove Cr(VI) ions by adsorption was experimentally demonstrated. The Fe incorporated in the gel showed strong affinity toward Cr(VI), with the maximum adsorption capacity of Fe-RF-AG found to be approximately 55 mg/g at 30°C at the aqueous phase concentration of 275 mg/l. The adsorption capacity significantly increased with decreasing pH. The numerical values of thermodynamic parameters, namely, ΔG (<0), ΔS (>0) and ΔH (>0) confirmed the spontaneous, irreversible and endothermic adsorption of Cr(VI) on Fe-RF-AGs, respectively. The prepared Fe-RF-AG aerogels may be potentially new alternative adsorbents for environmental remediation applications.

Acknowledgments: The authors are thankful to the Center for Environmental Science and Engineering at IIT Kanpur for carrying out the research.

References

[1] Izbicki JA, Ball JW, Bullen TD, Sutley SJ. *App. Geochem.* 2008, 23, 1325–1329.
[2] Sen M, Dastidar MG. *Iran J. Environ. Health Sci. Eng.* 2010, 7, 182–188.
[3] Costa M, Klein CB. *Crit. Rev Toxicol.* 2006, 36, 155–162.
[4] World Health Organization. *Guidelines for Drinking-Water Quality*, 3rd ed., Geneva, 2006.
[5] Rojas G, Silva J, Flores JA, Rodriguez A, Ly M, Maldonado H. *Sep. Purif. Technol.* 2005, 44, 31–36.
[6] Mohan D, Singh KP, Singh VK. *Ind. Eng. Chem. Res.* 2005, 44, 1027–1032.
[7] Vasudevan S, Lakshmi J, Vanathi R. *Clean* 2010, 38, 9–15.
[8] Vasudevan S, Lakshmi J. *Water Sci. Technol.* 2011, 11, 142–148.
[9] Vasudevan S, Lakshmi J, Sozhan G. *Desalination* 2012, 275, 260–270.
[10] Karthik R, Meenakshi S. *J. Water Process. Eng.* 2014, 1, 37–42.
[11] Mohan D, Pittman CU Jr. *J. Hazard Mater. B* 2006, 137, 762–766.
[12] Xu P, Zeng GM, Huang DL, Feng CL, Hu S, Zhao MH, Lai C, Wei Z, Huang C, Xie GX, Liu ZF. *Sci. Total Environ.* 2012, 424, 1–7.
[13] Li X, Cao J, Zhang W. *Ind. Eng. Chem. Res.* 2008, 47, 2131–2138.
[14] Qina G, Yaoa Y, Weib W, Zhangc T. *App. Surf Sci.* 2013, 280, 806–810.
[15] Meena AK, Mishra GK, Rai PK, Rajagopala C, Nagar PN. *J. Hazard. Mater.* 2005, 122, 161–168.
[16] Kadirvelu K, Goel J, Rajagopal C. *J. Hazard. Mater.* 2008, 153, 502–508.
[17] Sarawade PB, Kim J, Hilonga A, Kim HT. *Korean J. Chem. Eng.* 2010, 27, 1301–1306.
[18] Demirbas E, Kobya M, Senturk E, Ozkan T. *Water SA* 2004, 30, 533–539.
[19] Du A, Zhou B, Zhang Z, Shen J. *Materials* 2013, 6, 941–948.
[20] Merzbacher CI, Meier SR, Pierce JR, Korwin ML. *J. Non-Cryst. Solids*, 2001, 285, 210–215.
[21] Brandt R, Fricke J. *J. Non-Cryst. Solids* 2004, 350, 131–135.
[22] Barbieri O, Ehrburger-Dolle F, Rieker TP, Pajonk GM, Pinto N, Rao AV. *J. Non-Cryst. Solids* 2001, 285, 109–115.
[23] Pekala RW. *J. Mater. Sci.* 1989, 24, 3221–3226.
[24] Mulik S, Sotiriou-Leventis C, Leventis N. *Chem. Mater.* 2007, 19, 6138–6145.
[25] Czakkel O, Geissler E, Szilágyi IM, Székely E, László K. *J. Colloid. Interf. Sci.* 2009, 337, 513–518.
[26] Moreno-Castilla C, Maldonado-Hódar FJ, Pérez-Cadenas AF. *Langmuir* 2003, 19, 5650–5658.
[27] Tang L, Yang GD, Zeng GM, Cai Y, Li SS, Zhou YY, Pang Y, Liu YY, Zhang Y, Luna B. *Chem. Eng. J.* 2014, 239, 114–118.
[28] Eaton AD, Clesceri LS, Greenberg AE, Eds., *Standard Methods for the Examination of Water and Waste water*, 19th ed., Washington, DC: American Public Health Association American Water Works Association and Water Environment Federation, 1995.
[29] Talreja N, Kumar D, Verma N. *J. Water Process Eng*. 2014, 3, 34–45.
[30] Téllez GL, Díaz CEB, Hernández PB, Morales GR, Bilyeu B. *Chem. Eng. J.* 2011, 173, 480–485.
[31] Wang P, Lo IM. *Water Res.* 2009, 43, 3727–3734.
[32] Lv X, Xu J, Jiang G, Tang J, Xu X. *J. Colloid Interf. Sci.* 2012, 369, 460–469.
[33] Zelmanov G, Semiat R. *Sep. Puri. Tech.* 2011, 80, 330–337.
[34] Wei L, Yang G, Wang R, Ma W. *J. Hazard. Mater.* 2009, 164, 1159–1163.

Bionotes

Naveen Kumar Verma

Naveen Kumar Verma received his MTech degree from the Indian Institute of Technology Kanpur in 2014. His research interests include the development, characterization and application of novel carbon based materials for industrial, biological and environmental applications.

Prateek Khare

Prateek Khare is currently doing his PhD in the Department of Chemical Engineering at the Indian Institute of Technology Kanpur. His research interests include the development, characterization and application of novel carbon based materials for industrial, biological and environmental applications.

Nishith Verma

Nishith Verma received his PhD degree in Chemical Engineering from the University of Arizona, USA. After completing his PhD, he worked for 3 years with BOC Gases in New Jersey, USA before joining the Indian Institute of Technology Kanpur in 1998. He is presently the head of the Chemical Engineering Department and coordinator of the Center for Environmental Science and Engineering at IIT Kanpur. He has published more than 75 papers in reputed international journals and holds three patents. His research interests include adsorption, synthesis of carbon nanofibers and nanoparticles, environmental remediation, and transport modeling.